Available online at www.sciencedirect.com
SCIENCE DIRECT®
Physics and Chemistry of the Earth 31 (2006) 234–239
PHYSICS and CHEMISTRY of the EARTH
www.elsevier.com/locate/pce

An analysis of pressure stimulated currents (PSC), in marble samples under mechanical stress

D. Triantis [a,*], I. Stavrakas [a], C. Anastasiadis [a], A. Kyriazopoulos [b], F. Vallianatos [c]

[a] Department of Electronics, Technological Educational Institution of Athens, Ag Spiridonos street, Athens 122 10, Greece
[b] Department of Civil Engineering, Technological Educational Institution of Athens, Athens 122 10, Greece
[c] Department of Natural Resources and Environment, Technological Educational Institute of Crete, Chania, Crete 731 33, Greece

Accepted 6 February 2006
Available online 24 May 2006

Abstract

The pressure stimulated current (PSC) technique was used in two variations, LSRT and SST for the investigation of the relations governing stress rate dS/dt, electric charge release and the behaviour of the damage parameter D, when a rock sample is driven to fracture by application of uniaxial compressional stress. It was verified that PSC originates from the change in the Young's modulus rather than from the change in the stress rate. The total charge released during stress application up to fracture reaches almost the same values irrespectively of the stress rate, which is in full agreement with theory. It was also found that a proportionality exists between D and the scaling factor γ that correlates PSC peaks with the stress rate.

Keywords: Pressure stimulated currents; PSC; Marble; Damage parameter; Uniaxial stress

1. Introduction

The material fracture phenomena, particularly those concerning inhomogeneous materials, such as geomaterials, in association with transient electric phenomena, attract the interest of the scientific community. The main reason is that such phenomena are promising candidates of earthquake precursors (Hayakawa, 1999; Hayakawa and Fujinawa, 1994; Hayakawa and Molchanov, 2002; Freund, 2002). During the development of the geomaterial deformation, there appear mechanisms of generation of electric signal emission and a number of researchers acknowledge such mechanisms as related to crack generation and propagation in the Earth's crust (Molchanov and Hayakawa, 1995, 1998; Vallianatos and Tzanis, 1998; Tzanis et al., 2000). Although important similarities exist between the fracture of a pristine rock and an earthquake rupture, there are also important differences (Turcotte et al., 2003).

In order to understand the mechanisms that produce these electric signals, a number of laboratory experiments of mechanical stress up to sample fracture have been conducted on minerals and rocks (dry and saturated) (Nitsan, 1997; Ogawa and Miura, 1985; Enomoto and Hashimoto, 1990; Hadjicontis and Mavromatou, 1994; O'Keefe and Thiel, 1995; Takeuchi and Nagahama, 2001; Freund, 2000). The laboratory studies on emitted electric signals from rock specimens at the time of fracture, suggested that these signals are produced by the piezoelectric effect of quartz (e.g., Nitsan, 1997), electrokinetic effect due to water movement (e.g., Ishido and Mizutani, 1981), point defects (Varotsos and Alexopoulos, 1986; Hadjicontis and Mavromatou, 1994), emission of electrons (Brady and Rowell, 1986; Enomoto and Hashimoto, 1990), and recently by moving charged dislocations (Molchanov and Hayakawa, 1995; Vallianatos and Tzanis, 1998; Tzanis and Vallianatos, 2002).

* Corresponding author. Tel./fax: +0030 210 5316525.
E-mail address: triantis@ee.teiath.gr (D. Triantis).

1474-7065/$ - see front matter © 2006 Elsevier Ltd. All rights reserved.
doi:10.1016/j.pce.2006.02.018

Recently in a series of laboratory experiments conducted on marble samples, we have confirmed that the application of a uniaxial stress is accompanied by the production of weak electric currents that have been described by the term pressure stimulated currents (PSC) (Stavrakas et al., 2003, 2004; Vallianatos et al., 2004; Anastasiadis et al., 2004).

In the present work, we will consider an analysis of PSC recordings that occur during experiments on different applied stress modes. The results obtained under different stress applications are discussed. A correlation of the amplitude of the emitted PSC to the damage parameter under abrupt stress application becomes evident.

2. Experimental techniques for PSC recording

There are two main experimental techniques for detecting emitted PSC when applying uniaxial compressional stress. The difference between these techniques is in the temporal variation of the stress rate.

In the former technique, the uniaxially applied stress is increasing linearly (i.e., at a constant rate) according to

$$S = a \cdot t$$

where a is the stress rate. When $t = t_f = S_{\max}/a$, where $S_{\max}$ stands for the ultimate compressional stress strength, the sample fails. In a significant number of previous experiments by Stavrakas et al. (2003, 2004), the stress rate, a, has been varying between 0.1 and 0.3 MPa/s depending on the fracture limit of the geomaterial. This experimental technique, henceforth, will be referred to as low stress rate technique (LSRT).

In the latter technique and while the sample is suffering a constant uniaxial stress (S_k), an abrupt step-like stress increase is applied for a short period Δt and $\Delta S = S_{k+1} - S_k$ where S_{k+1} is the final state of the applied stress increase. We note that the final stress state S_{k+1} is constant until a following stress increase is applied (see Fig. 1).

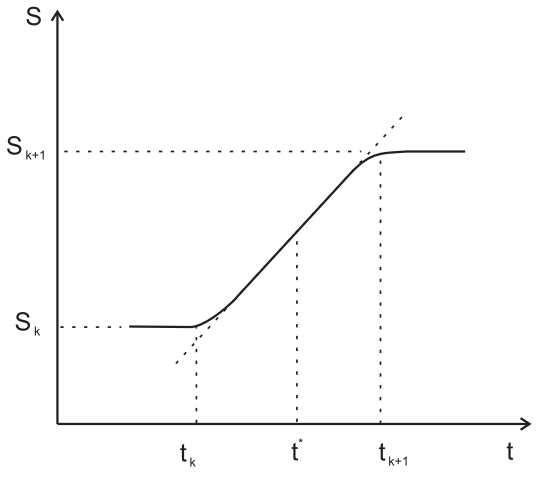

Fig. 1. Description of the step like increase of the uniaxial compressional stress.

The aforementioned temporal variation of the stress, S, as recorded during this experimental procedure can be described in a good approximation by the following equation.

$$S(t) = \begin{cases} S_k = \text{constant} & \text{for } t < t_k \\ S_k + b(t - t_k) & \text{for } t_k < t < t_{k+1} \\ S_{k+1} = \text{constant} & \text{for } t > t_{k+1} \end{cases}$$

A good estimation of the stress rate, b, could be obtained experimentally near $t^* = (t_k + t_{k+1})/2$. This step-like stress technique hereafter called SST is important to expose PSC in both elastic and plastic deformation ranges of the material deformation. Typical values of the stress rate, b, are always greater than those of the stress rate, a, of the LSRT technique.

3. Theoretical remarks

The stress, S, on the material is given as a function of the strain, ε. For the linear elasticity range it can be stated that

$$S = Y_0 \cdot \varepsilon \tag{1}$$

where Y_0 is the Young's modulus of the undamaged material which is constant in the elastic range. When the stress takes values that lead further than the (linear) elastic range then microcracks occur. For a prescribed stress, S, the strain, ε, is greater than the value given by Eq. (1). Accordingly, we write (Turcotte et al., 2003)

$$S = Y_{\text{eff}} \cdot \varepsilon \tag{2}$$

where Y_{eff} is the effective Young's modulus and it is no longer considered as constant. In the plastic range the Young's modulus becomes progressively smaller while stress increases. An approach to this process is to introduce a damage parameter, D, so that (Krajcinovic, 1996; Lemaitre and Chaboche, 1990)

$$Y_{\text{eff}} = Y_0(1 - D) \tag{3}$$

The damage parameter, D, quantifies the deviation from linear elasticity, thus describing the rate of generation of microcracks. In general $0 < D < 1$. When $D = 0$, linear elasticity is obtained with Eq. (1) valid, but when $D = 1$, failure occurs. The damage parameter depends mainly on the applied stress $D(S)$.

During an abruptly increasing stress on a brittle material a theoretical model has been qualitatively described by Slifkin (1993) and further developed by Vallianatos and Tzanis (1998, 1999) and Tzanis and Vallianatos (2002) in order to explain current production due to stress in non-piezoelectric and non-electrokinetic materials. The model is met in the literature as moving charged dislocations model (MCD). According to this model the observed transient electric variation is related to the non-stationary accumulation of deformation. The expected emission of pressure stimulated current, I, is proportional to the strain rate, $(d\varepsilon/dt)$. Thus

(i) if the Young's modulus $Y = Y_0 = \text{constant}$ (see Eq. (1)) then

$$I \propto \frac{dS}{dt} \tag{4}$$

(ii) if $Y = Y_{\text{eff}}$ (see Eqs. (2) and (3)) then

$$I \propto \frac{1}{Y_{\text{eff}}}\frac{dS}{dt} \propto \frac{1}{1-D}\frac{dS}{dt} \tag{5}$$

Based on the above, when the LSRT technique ($dS/dt = a = \text{constant}$) is applied and Eq. (1) is valid no significant transient PSC should be observed. When the stress exceeds the elastic limit (see Eq. (2)), microcracks (i.e. damage) begin to form; further increase of the stress causes the microcracks to multiply and propagate while the material deforms non-elastically and PSC emission is detected. When applying the SST technique, it is possible to detect PSC even in the case where the geomaterial is stressed in the linear range. This can be done for high stress rates.

When the technique is applied in the non-linear range (Eqs. (2) and (3) valid) PSC is emitted and its magnitude is a function of the damage parameter, D, (see Eq. (5)).

4. Experimental details

In the described experiment, Dionysos marbles collected from Mt. Penteli, Attica were used. The Dionysos marble is mainly composed of calcite (98%) and other minerals (2% approximately). Its content in quartz is very low, about 0.2%. Its density is 2.7 g/cm^3 and its porosity is approximately 0.4%.

Table 1 contains the characteristics of the samples used for the experiments as well as a short description of each experimental technique followed. The sample code corresponds to the following information. The MD corresponds to Dionysos Marbles the number that follows describes the rock mass that the samples were extracted from. The last letter encodes each sample separately.

The stressing system comprised a uniaxial hydraulic load machine (Enerpac–RC106) that applied compressional stress to the sample. For conducting the electrical measurements of PSC recordings, a sensitive programmable electrometer (Keithley 617) was used. The experimental setup of the applied technique as well as the procedure of PSC recording has been described in previous works by Stavrakas et al. (2003) and Anastasiadis et al. (2004).

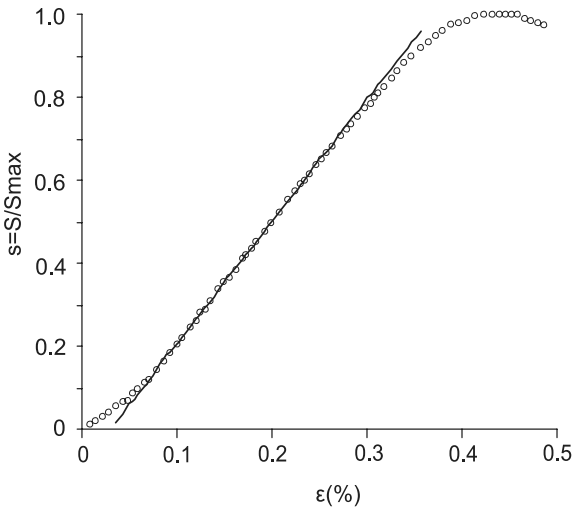

Fig. 2. Stress–strain curve for marble samples on normalised stress axis.

The stress–strain curve of Fig. 2 corresponds to the marble samples used and depicts the normalised stress, $s = S/S_{\max}$, where $S_{\max}$ corresponds to the ultimate compressional stress strength as a function of strain, ε. It is noted that when normalised stress exceeds the limiting value $s = 0.65$ approximately the material has practically abandoned the (linear) elastic range where the Young's modulus becomes progressively smaller when stress increases. This process goes for normalised stress values even beyond $s = 0.98$ where the fracture plane is defined (Agioutantis, 2002).

5. Results and discussion

The experimental results of the LSRT technique are presented and discussed for the two samples encoded as MD01a and MD01b that suffered stress at different rates (see Table 1). Fig. 3 shows the PSC emitted from the two samples. Both PSC emissions initiate when the normalised stress values are approximately in the range $s \approx 0.65$–0.70, which is in accordance with Eq. (5) stating that PSC variations are detected due to the change of Young's modulus despite the fact that dS/dt is constant. At the moment of fracture of the sample MD01a the emitted PSC reached a greater value (410 pA) than the corresponding PSC of the sample MD01b (340 pA). Despite that, it is important to mention that the total charge released during the stress

Table 1
The characteristics of the used samples

Sample code	Sample dimensions (mm)	$S_{\max}$ (MPa)	Experimental technique
MD01a	$69.6 \times 49.0 \times 109.1$	72	LSRT, $a = 144$ kPa/s
MD01b	$69.8 \times 48.9 \times 108.8$	75	LSRT, $a = 93$ kPa/s
MD02	$69.6 \times 49.0 \times 61.2$	72	Multiple SST with rate 0.6 MPa/s $< b <$ 1.6 MPa/s

It is noted that the sample MD02 suffered various SST mode stress steps mainly in the non-linear range. The stress rate, b, varied in the range 0.6–1.6 MPa/s.

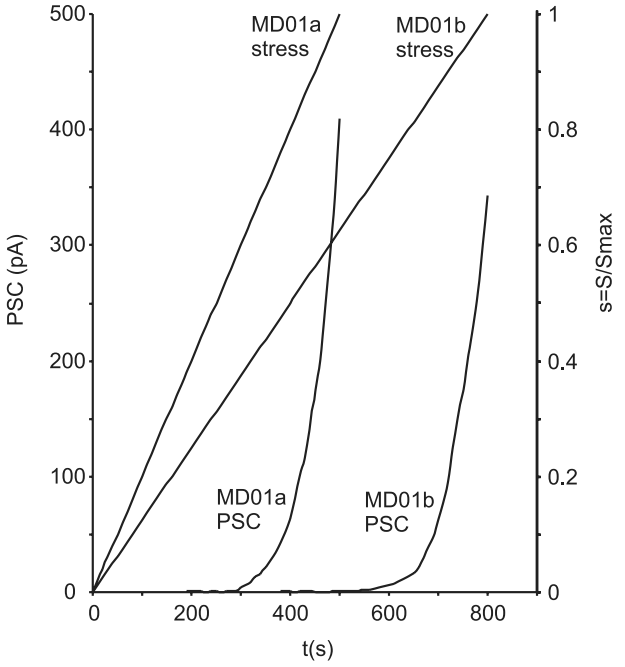

Fig. 3. The temporal development of the normalised stress when the stress rate was constant with respect to the corresponding PSC emitted.

application up to fracture reaches almost the same values, if the total charge released, Q, is calculated according to

$$Q = \int_{t_0}^{t_f} i(t)\mathrm{d}t \tag{6}$$

where t_0, is the moment when PSC initiates, and t_f the moment of fracture, the values of the charge are 21.9 pC and 20.8 pC for the samples MD01a and MD01b, respectively. According to Eq. (5)

$$I = \frac{k}{1-D}\frac{\mathrm{d}S}{\mathrm{d}t},$$

where $0 \leqslant D(S) \leqslant 1$, and substituting Eq. (3) into Eq. (6) gives that the total charge released is

$$Q = k \cdot \int_{S_p}^{S_{\max}} \frac{\mathrm{d}S}{1-D(S)} \tag{7}$$

where S_p corresponds to the stress value that the material enters the plastic deformation range. According to Shcherbakov and Turcotte (2003) when the applied stress, S, increases linearly with time the plot of $\log(1-D)$ versus $\log(1-t/t_f)$ has a straight line behavior indicating a power-law scaling, which is very close to the power 1/3. Thus, the stress evolution of the damage parameter $D(S)$ is given by an expression

$$D(S) = 1 - A \cdot (S_{\max} - S)^a \tag{8}$$

where $a \approx \frac{1}{3}$ and $S_p \leqslant S \leqslant S_{\max}$.

It is obvious that since $D(S) = 0$ when $S = S_p$, $A = (S_f - S_p)^{-a}$. Combining Eqs. (7) and (8) and calculating the integral

$$Q = \frac{k \cdot S_{\max}}{1-a}\left(1 - \frac{S_p}{S_{\max}}\right) \tag{9}$$

Eq. (9) states that in the frame of self-similarity of fracture introduced by Shcherbakov and Turcotte (2003) and Turcotte et al. (2003), the charge released by using the LSRT technique depends on the failure stress $S_{\max}$ and the ratio $S_p/S_{\max}$, which is the transition point from linear to plastic range.

It is obvious that since $S_{\max} \approx 72$–75 MPa and $S_p/S_{\max} \approx 0.65$–$0.70$ for the marble samples, the total charge released, Q, has to be constant, as the LSRT experiments suggest.

Regarding the SST experiment, the marble rock sample was subjected to five uniaxial stress steps, which correspond to a range of normalised stress from 0.51 to 0.94. Fig. 4 shows the five uniaxial stress steps with respect to time and the corresponding PSC recordings during the uniaxial stress increase, as well as while the uniaxial stress was kept at the high stress level. The stress is maintained on the sample with the high stress level lasting at least for the time needed for the PSC to be eliminated (background current).

The first uniaxial stress step applied corresponds to a level of normalised stress of $0.51 < s < 0.62$. This range corresponds to the material linear part of mechanical behaviour and is close to the non-linearity low limit. The average normalised stress rate of this stress step was $0.022\ \mathrm{s}^{-1}$ and the recorded PSC peak maximum read was $I_{\max} = 0.15$ pA. Afterwards, four more uniaxial stress steps were applied (see Fig. 4), and their characteristics are described in Table 2. In the same table the characteristics of the recorded PSC (i.e. $I_{\max}$, etc.) are also included. Since the five steps have different stress rates ($\mathrm{d}s/\mathrm{d}t$) a comparison of the peaks, $I_{\max}$, can be made if a scaling factor, γ, is introduced.

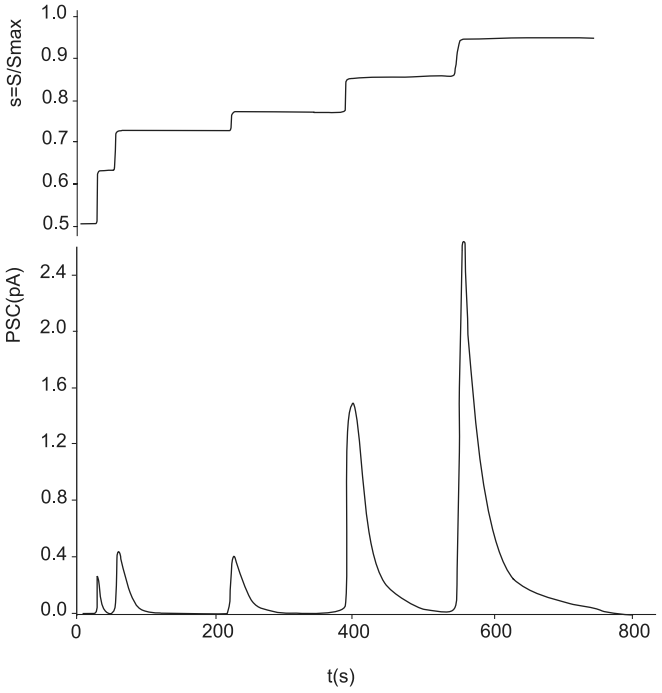

Fig. 4. The uniaxial stress steps and the corresponding PSC recordings with respect to time, in the range $0.51 < s < 0.94$.

Table 2
Characteristics of the stress steps and the PSC peaks of Fig. 4

	1st step	2nd step	3rd step	4th step	5th step
Normalised stress range	0.51–0.62	0.62–0.72	0.73–0.76	0.76–0.85	0.84–0.94
$\langle ds/dt\rangle$ (s^{-1})	0.022	0.020	0.011	0.016	0.0085
I_{max} (pA)	0.31	0.48	0.42	1.58	2.62
Factor γ (pC)	14.3 ± 0.9	24 ± 1.0	38 ± 2.0	98 ± 7	309 ± 20
Parameter D	0.0	0.015 ± 0.003	0.033 ± 0.005	0.1 ± 0.01	0.3 ± 0.05

$$\gamma = \frac{I_{max}}{\langle ds/dt\rangle} \tag{10}$$

The corresponding values of γ for the five steps are included in Table 2.

The calculation error of the average stress rate of each step $\langle dS/dt\rangle$ for the conducted experiments is estimated to be around 5–7%. Consequently, the error of the γ factor calculation cannot be greater than 10% since PSC recording error is lower than 1%. Table 2 also includes the calculated error of γ factor estimation.

An attempt is made to evaluate Eq. (5) on the basis of the MCD model. The damage parameter calculation can be done by using Eq. (3) and the stress–strain curve of marble (Fig. 2). Calculations show that for the used samples the damage parameter becomes greater than zero, $D \geqslant 0$, when the normalised stress reaches values greater than 0.65 approximately. When the normalised stress becomes greater than 0.65 the damage parameter continuously increases and for $s = 0.94$ it tends to $D \approx 0.3$. For each stress step the parameter D is calculated including the relevant error, given that each step corresponds to a normalised stress range (see row 1 in Table 2).

According to Eq. (5) the scaling factor, γ, is proportional of the quantity $\frac{1}{1-D}$. Based on the values of Table 2, Fig. 5 depicts the dependence of the scaling factor, γ, on the quantity $\frac{1}{1-D}$. A clear linear relationship is evident between the two quantities, which is cancelled for high stress values in the vicinity of fracture where parameter D reaches values greater than 0.3.

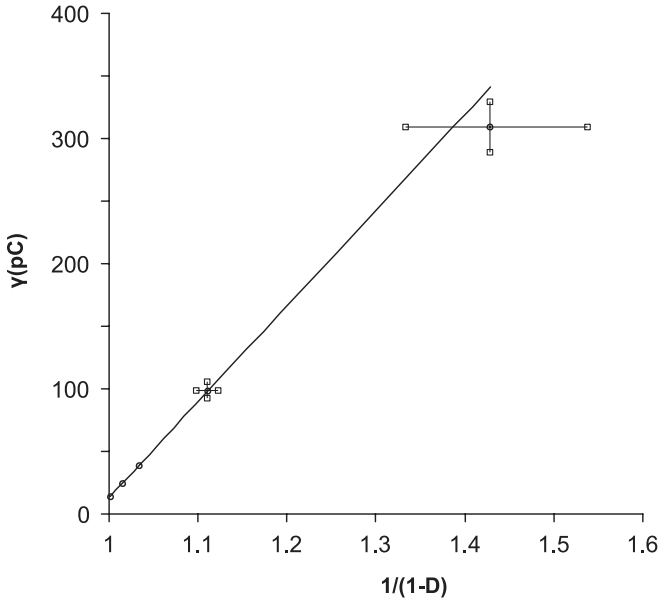

Fig. 5. The values of scaling factor γ with respect to the quantity $(1/1 - D)$. The best fitted line is also presented.

6. Concluding remarks

The main conclusions of this work can be summarized in the following points.

1. Any external stimulation originated by either gradual or fast stress increase (i.e. stress step) on rock samples results in PSC emission. The time recording of PSC shows a peak during the completion of the applied stress step. After the peak, the PSC relaxes slowly to the background noise level. This relaxation process takes place while the stress is maintained at the higher stress level of each step.
2. As a result of the LSRT technique, it was found that PSC originates from the change in the Young's modulus rather than from the change in the stress rate.
3. While using the LSRT technique, the total charge released during stress application up to fracture reaches almost the same values irrespectively of the stress rate. This is in full agreement with theory.
4. An obvious proportionality seems to exist between the damage parameter, D, that quantifies the deviation from linear elasticity of the sample and the scaling factor, γ, that correlates each PSC peak with the corresponding normalised stress rate, thus, the damage variable is related to the stress rate.

Acknowledgement

This work is supported by the project ARCHIMEDES II: 'Support of Research Teams of Technological Educational Institute of Athens', sub-project entitled 'The electric behavior of geo-materials' in the framework of the Operational Programme for Education and Initial Vocational Training. It is co-funded by 75% by the EU and 25% by the Greek Government.

References

Agioutantis, Z., 2002. Elements of Geomechanics–Rock Mechanics. Ion Publishing, Athens, in Greek.

Anastasiadis, C., Triantis, D., Stavrakas, I., Vallianatos, F., 2004. Pressure stimulated currents (PSC) in marble samples after the

application of various stress modes before fracture. Ann. Geophys. 47 (1), 21–28.
Brady, B.T., Rowell, G.A., 1986. Laboratory investigation of the electrodynamics of rock fracture. Nature 321, 448–492.
Enomoto, J., Hashimoto, H., 1990. Emission of charged particles from indentation fracture of rocks. Nature 346, 641–643.
Freund, F., 2000. Time-resolved study of charge generation and propagation in igneous rocks. J. Geophys. Res. B105, 11001–11019.
Freund, F., 2002. Charge generation and propagation in igneous rocks. J. Geodynam. 33, 543–570.
Hadjicontis, V., Mavromatou, C., 1994. Transient electric signals prior to rock failure under uniaxial compression. Geophys. Res. Lett. 21, 1687–1690.
Hayakawa, M. (Ed.), 1999. Electromagnetic Phenomena Related to Earthquake Prediction. Terra Scientific Publishing Company, Tokyo.
Hayakawa, M., Fujinawa, Y. (Eds.), 1994. Electromagnetic Phenomena Related to Earthquake Prediction. Terra Scientific Publishing Company, Tokyo.
Hayakawa, M., Molchanov, O.A. (Eds.), 2002. Seismo Electromagnetics: Lithosphere–Atmosphere–Ionosphere Coupling. Terra Scientific Publishing Company, Tokyo.
Ishido, T., Mizutani, H., 1981. Experimental and theoretical basis of electrokinetic phenomena in rock–water systems and its applications to geophysics. J. Geophys. Res. 86, 1763–1775.
Krajcinovic, D., 1996. Damage Mechanics. Elsevier, Amsterdam.
Lemaitre, J., Chaboche, J.L., 1990. Mechanics of Solid Materials. Cambridge University Press, Cambridge.
Molchanov, O.A., Hayakawa, M., 1995. Generation of ULF electromagnetic emissions by microfracturing. Geophys. Res. Lett. 22, 3091–3094.
Molchanov, O.A., Hayakawa, M., 1998. On the generation mechanism of ULF seismogenic electromagnetic emissions. Phys. Earth Planet. Int. 105, 201–210.
Nitsan, U., 1997. Electromagnetic emission accompanying fracture of quartz-bearing rocks. Geophys. Res. Lett. 4, 333–337.
Ogawa, T.K., Miura, T., 1985. Electromagnetic radiation from rocks. J. Geophys. Res. 90, 6245–6249.
O'Keefe, S.G., Thiel, D.V., 1995. A mechanism for the production of electromagnetic radiation during fracture of brittle materials. Phys. Earth Planet. Int. 89, 127–135.
Shcherbakov, R., Turcotte, D.L., 2003. Damage and self-similarity in fracture. Theor. Appl. Fract. Mech. 39, 245–258.
Slifkin, L., 1993. Seismic electric signals from displacement of charged dislocations. Tectonophysics 224, 149–152.
Stavrakas, I., Anastasiadis, C., Triantis, D., Vallianatos, F., 2003. Piezo stimulated currents in marble samples: Precursory and concurrent – with – failure signals. Nat. Hazards Earth Syst. Sci. 3, 243–247.
Stavrakas, I., Triantis, D., Agioutantis, Z., Maurigiannakis, S., Saltas, V., Vallianatos, F., Clarke, M., 2004. Pressure stimulated currents in rocks and their correlation with mechanical properties. Nat. Hazards Earth Syst. Sci. 4, 563–567.
Takeuchi, A., Nagahama, H., 2001. Voltage changes induced by stick-slip of granites. Geophys. Res. Lett. 28, 3365–3367.
Turcotte, D.L., Newman, W.I., Shcherbakov, R., 2003. Micro and macroscopic models of rock fracture. Geophys. J. Int. 152, 718–728.
Tzanis, A., Vallianatos, F., 2002. A physical model of electrical earthquake precursors due to crack propagation and the motion of charged edge dislocations. In: Hayakawa, M., Molchanov, O.A. (Eds.), Seismo Electromagnetics: Lithosphere–Atmosphere–Ionosphere Coupling. Terra Scientific Publishing Company, Tokyo, pp. 117–130.
Tzanis, A., Vallianatos, F., Gruszow, S., 2000. Identification and discrimination of transient electrical earthquake precursors: Fact, fiction and some possibilities. Phys. Earth Planet. Int. 121, 223–248.
Vallianatos, F., Tzanis, A., 1998. Electric current generation associated with the deformation rate of a solid: Preseismic and coseismic signals. Phys. Chem. Earth 23, 933–938.
Vallianatos, F., Tzanis, A., 1999. A model for the generation of precursory electric and magnetic fields associated with the deformation rate of the earthquake focus. In: Hayakawa, M. (Ed.), Atmospheric and Ionospheric Electromagnetic Phenomena Associated with Earthquakes. Terra Scientific Publishing Company, Tokyo, pp. 287–305.
Vallianatos, F., Triantis, D., Tzanis, A., Anastasiadis, C., Stavrakas, I., 2004. Electric earthquake precursors: From laboratory results to field observations. Phys. Chem. Earth 29, 339–351.
Varotsos, P., Alexopoulos, K., 1986. Thermodynamics of point defects and their relation with bulk properties, vol. 474. North-Holland, Amsterdam.